Modal characteristics of in-plane vibration of circular plates clamped at the outer edge

N. H. Farag and J. Pan
School of Mechanical Engineering, The University of Western Australia, 35 Stirling Highway, Crawley, Western Australia 6009, Australia

(Received 11 January 2002; revised 13 December 2002; accepted 16 December 2002)

The equations of in-plane vibration in thin flat plates are solved for free vibration in circular plates clamped at the outer edge. The mode shapes are represented by trigonometric functions in the circumferential direction and by series summation of Bessel functions in the radial direction. Accuracy of the predictions of natural frequencies and mode shapes is assessed by comparisons with finite-element predictions and with previously reported results. The present solution gives very accurate predictions. The work also highlights the nature of coupling between the different circumferential and radial modes and the response of different vibrational modes at the center of the plate. It is shown that the center point of the plate vibrates only for modes with unity circumferential wave number (number of nodal diameters). Nondimensional frequency parameters are listed and the radial mode shapes of natural vibration are depicted to illustrate the free-vibration behavior in the frequency range of practical interest.
[DOI: 10.1121/1.1553456]

PACS numbers: 43.40.Dx [ANN]

LIST OF SYMBOLS AND BASIC RELATIONS

E	Young's modulus of elasticity
h	plate thickness
j	the imaginary number $\sqrt{-1}$
m	circumferential wave number (equals number of nodal diameters)
N_{rr}, $N_{\theta\theta}$, $N_{r\theta}$	in-plane force components (force per unit length) in the directions shown in Fig. 1
$\overline{r}$	plate radius
u, v	components of in-plane displacement in radial (extensional) and circumferential (torsional) directions, respectively
f	frequency (Hz)
ω	angular frequency (radians per second)
ν	Poisson's ratio
ρ	mass density
$C_L^2 = E/\varrho(1-\nu^2)$	square of the quasilongitudinal wave speed in the plate
$C_T^2 = E/2\varrho(1+\nu)$	square of the in-plane shear wave speed in the plate
$K_L = \omega\overline{r}/C_L$	nondimensional frequency parameter

I. INTRODUCTION

Circular plates exist in many engineering applications. In particular, they form partitions in aircraft fuselages and external fuel tanks and end plates in storage tanks. Some of these applications are subjected to dynamic excitations with large components lying in the middle plane of the plate. The in-plane dynamic loads, being continuous, intermittent, or even impacts, will excite in-plane modes with resonance frequencies in the frequency bands of excitation.

Investigation of the free in-plane vibrational response in circular thin flat plates with clamped edge is the subject of this work. The main objective is to provide the structural dynamics analyst with a quick and easy tool to predict in-plane natural frequencies and depict their mode shapes, and to reveal some important aspects of modal characteristics of in-plane vibration.

While much work has been done on the investigation and documentation of the natural frequencies and modes shapes for flexural vibration (e.g., Refs. 1 and 2), the characteristics of in-plane vibration have not been completely investigated and are not well documented. However, increasing attention has been given to the in-plane vibration in single and complex plate and plate-like structures in the past few years (e.g., Refs. 3–7). The results of recent investigations emphasize the importance of the in-plane response at high frequencies and in large coupled plate-like structures.

Predictions of the natural frequencies of circular plates are treated in few references. In particular, the problems of in-plane vibration and stability of rotating disks have attracted attention of researchers for decades due to their obvious practical importance in many engineering applications. Also, the in-plane vibrational response was investigated for piezoelectric disks and computer disks. These investigations have been dealing with circular and annular thin or thick plates. Free-boundary conditions at the plate edge(s) were considered in most of the published work.

Holland[8] investigated the free in-plane vibration in circular plates with free edges using trigonometric and Bessel functions and published frequency parameters for five to ten modes of the first nine circumferential modes (circumferential wave numbers $m=1$ to 9) for different values of Pois-

son's ratio. Ambati *et al.*[9] examined the in-plane vibrations in circular and annular plates, and rings with free boundaries. Irie *et al.*[10] used a transfer matrix formulation to solve the equations of free in-plane vibrations for the natural frequencies of annular plates with combinations of free and clamped conditions at the inner and outer edges. In Ref. 10, the circular plate was considered as a limiting case when the inner diameter tends to zero. For this specific case of circular plates, the frequency parameters (nondimensional natural frequencies) are listed for the first two radial modes of five circumferential wave numbers ($m=0$ to 4). The mode shapes were not examined in Ref. 10. The first eight references sited in Ref. 10 represent the bulk of the work done on in-plane free vibration of annular and circular thin plates up to 1984. Chen *et al.*[11] presented displacement potentials' formulation to examine the effect of the angular velocity of spinning disks on the in-plane vibrations and natural frequencies.

To conclude, it can be seen that limited work is reported on the in-plane vibration of circular clamped plates. This type of structure was only considered as a limited case of annular plate when the inner radius goes to zero[10] and the radial mode shapes of in-plane vibration have not been reported.

The present work is a comprehensive investigation of the modal characteristics of in-plane vibration in circular plates with clamped edge (i.e., rigidly restrained edge in the plane of the plate). It concentrates on the following new areas: (i) The circular plate is investigated directly not as a special case of annular plate when the inner radius goes to zero. (ii) The work clarifies the modal response at the plate center and the nature of the coupling between different circumferential modes and different radial modes. (iii) The mode shapes of in-plane vibration in the radial direction are examined in detail. (iv) Nondimensional frequency parameters and mode shapes are tabulated. (v) Elements of the characteristic equation are presented, which can be used to compute the natural frequencies and mode shapes for other material properties or higher frequency ranges.

In this paper, the equations for in-plane free vibration are presented in polar coordinates suitable for the type of structure under investigation. Assumed mode shapes are expressed in terms of trigonometric functions in the circumferential direction. The nature of coupling between the circumferential modes is investigated. The physical behavior of the center point of the plate, during free vibration in each of the circumferential modes, is examined. Mode shapes in the radial direction are assumed as series summation of Bessel functions. The mathematical model for free vibration is written in the form of an eigenvalue problem so that natural frequencies and modes shapes can be obtained by solving for eigenvalues and eigenvectors employing any available mathematical software. The frequency parameters obtained by the present method are tabulated and the mode shapes are depicted to illustrate the free-vibration behavior in the frequency range of practical interest. Comparisons with finite-element results and with the previously reported results confirm the accuracy of the predictions of the present method. The effect of Poisson's ratio on the natural frequencies is also examined.

The mathematical formulations are presented in Sec. II followed by computational examples and discussions in Sec. III. Tables I and II include a tabulation of the frequency parameters and mode shape functions for in-plane vibration in circular clamped plates.

II. MATHEMATICAL SOLUTIONS FOR FREE IN-PLANE VIBRATION IN CIRCULAR CLAMPED PLATES

In this section the equations of free in-plane vibration, in polar coordinates, are presented. The assumed solution represents the circumferential distribution of in-plane vibration by cosine/sine functions and the radial distribution by series summation of Bessel functions. The coupling between the circumferential modes is investigated, as well as their response at the center point of the circular plate. Suitable mathematical forms of the radial mode shapes are used accordingly. The assumed modal response is substituted into the equations of motion. After mathematical manipulation the equations are presented in the form of eigenvalue problems suitable for solution for the nondimensional frequency parameters and mode shapes.

A. Equations of motion

The equations governing free in-plane vibration of thin flat plates, in polar coordinates, can be found in many references (e.g., Refs. 10 and 11). They may be written in the following form:

$$\frac{\partial^2 u}{\partial t^2}-C_L^2\left[\frac{\partial^2 u}{\partial r^2}+\frac{1}{r}\frac{\partial u}{\partial r}-\frac{u}{r^2}\right]-C_T^2\frac{1}{r^2}\frac{\partial^2 u}{\partial \theta^2}-C_T^2\frac{1}{r}\frac{1+v}{1-v}\frac{\partial^2 v}{\partial r\,\partial\theta}+C_T^2\frac{1}{r^2}\frac{3-v}{1-v}\frac{\partial v}{\partial\theta}=0, \tag{1a}$$

$$\frac{\partial^2 v}{\partial t^2}-C_T^2\left[\frac{\partial^2 v}{\partial r^2}+\frac{1}{r}\frac{\partial v}{\partial r}-\frac{v}{r^2}\right]-C_L^2\frac{1}{r^2}\frac{\partial^2 v}{\partial \theta^2}-C_T^2\frac{1}{r}\frac{1+v}{1-v}\frac{\partial^2 u}{\partial r\,\partial\theta}-C_T^2\frac{1}{r^2}\frac{3-v}{1-v}\frac{\partial u}{\partial\theta}=0. \tag{1b}$$

Please see the list of symbols at the beginning of the paper. The above equations are based on the assumptions of thin plate theory[1] and plane stress conditions.[8] The positive directions of displacement and internal force components are illustrated in Fig. 1.

The in-plane internal force intensities (force per unit length perpendicular to the force direction) are expressed in terms of displacements by the following relations:[10]

$$N_r=\frac{-Eh}{1-\nu^2}\left(\frac{\partial u}{\partial r}+\frac{\nu}{r}\frac{\partial v}{\partial\theta}+\frac{\nu}{r}u\right), \tag{2a}$$

$$N_\theta=\frac{-Eh}{1-\nu^2}\left(\frac{1}{r}\frac{\partial v}{\partial\theta}+\frac{u}{r}+\nu\frac{\partial u}{\partial r}\right), \tag{2b}$$

$$N_{r\theta}=\frac{-Eh}{2(1+\nu)}\left(\frac{1}{r}\frac{\partial u}{\partial\theta}+\frac{\partial v}{\partial r}-\frac{v}{r}\right). \tag{2c}$$

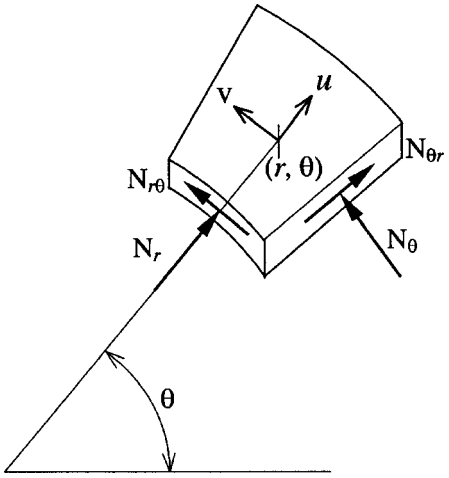

FIG. 1. Positive directions of in-plane force and displacement components on an infinitesimal element of a circular plate.

For harmonic vibration with time dependence $e^{-j\omega t}$, the free in-plane vibrational response is assumed in the form

$$u(r,\theta,t)=\sum_{m_1=0}^{\infty} U_{m1}(r)\cos(m_1\theta)e^{-j\omega t}, \tag{3a}$$

$$v(r,\theta,t)=\sum_{m_2=0}^{\infty} V_{m2}(r)\sin(m_2\theta+\varphi)e^{-j\omega t}. \tag{3b}$$

The angle φ is introduced in Eq. (3b) to accommodate a nonzero response $v(r,\theta,t)$ for the case of $m_2=0$. Therefore, $\varphi=\pi/2$ for $m_2=0$ and $\varphi=0$ for all other values of m_2.

The following equations are obtained after substitution of the assumed solution from Eqs. (3) into Eqs. (1), multiplying the resulting two equations by $\cos(m_1\theta)$ and $\sin(m_2\theta+\varphi)$, respectively, integrating with respect to θ from $\theta=0$ to $\theta=2\pi$, and employing the orthogonal properties of the trigonometric functions

$$C_L^2\frac{\partial^2 U_{m_1}}{\partial r^2}+C_L^2\frac{1}{r}\frac{\partial U_{m_1}}{\partial r}+\left(\omega^2-\frac{C_L^2+m_1^2C_T^2}{r^2}\right)U_{m_1}$$
$$+C_T^2\frac{1+v}{1-v}\frac{1}{r}\frac{1}{\pi}\sum_{m_2=0}^{\infty} I_{m_2,m_1}\frac{\partial V_{m_2}}{\partial r}$$
$$-C_T^2\frac{3-v}{1-v}\frac{1}{r^2}\frac{1}{\pi}\sum_{m_2=0}^{\infty} I_{m_2,m_1}V_{m_2}=0, \tag{4a}$$

$$C_T^2\frac{\partial^2 V_{m_2}}{\partial r^2}+C_T^2\frac{1}{r}\frac{\partial V_{m_2}}{\partial r}+\left(\omega^2-\frac{C_T^2+m_2^2C_L^2}{r^2}\right)V_{m_2}$$
$$-C_T^2\frac{1+v}{1-v}\frac{1}{r}\frac{1}{\pi}\sum_{m_1=0}^{\infty} I_{m_1,m_2}\frac{\partial U_{m_1}}{\partial r}$$
$$-C_T^2\frac{3-v}{1-v}\frac{1}{r^2}\frac{1}{\pi}\sum_{m_1=0}^{\infty} I_{m_1,m_2}U_{m_1}=0, \tag{4b}$$

where

$$I_{m_1,m_2}=m_1\int_0^{2\pi}\sin(m_1\theta)\sin(m_2\theta+\varphi)\,d\theta$$
$$=\begin{cases}0 & \text{for } m_1\neq m_2\\ m_1\pi\cos\varphi & \text{for } m_1=m_2\end{cases}, \tag{5a}$$

$$I_{m_2,m_1}=m_2\int_0^{2\pi}\cos(m_2\theta+\varphi)\cos(m_1\theta)\,d\theta$$
$$=\begin{cases}0 & \text{for } m_1\neq m_2\\ m_2\pi\cos\varphi & \text{for } m_1=m_2\end{cases}. \tag{5b}$$

Equations (4) and (5) indicate that $m_1=m_2=m$ is the condition for u and v to be coupled. The governing equations of free vibration take the following form for coupled circumferential modes:

$$C_L^2\frac{\partial^2 U_m}{\partial r^2}+C_L^2\frac{1}{r}\frac{\partial U_m}{\partial r}+\left(\omega^2-\frac{C_L^2+m^2C_T^2}{r^2}\right)U_m$$
$$+C_T^2\frac{1+v}{1-v}\frac{m}{r}\frac{\partial V_m}{\partial r}-C_T^2\frac{3-v}{1-v}\frac{m}{r^2}V_m=0, \tag{6a}$$

$$C_T^2\frac{\partial^2 V_m}{\partial r^2}+C_T^2\frac{1}{r}\frac{\partial V_m}{\partial r}+\left(\omega^2-\frac{C_T^2+m^2C_L^2}{r^2}\right)V_m$$
$$-C_T^2\frac{1+v}{1-v}\frac{m}{r}\frac{\partial U_m}{\partial r}-C_T^2\frac{3-v}{1-v}\frac{m}{r^2}U_m=0. \tag{6b}$$

Using the nondimensional parameter $x=r/\bar{r}$, where $\bar{r}$ is the outer radius of the circular plate, and the relation $C_T^2=[(1-\nu)/2]C_L^2$, the above equations take the form

$$x^2U_m''(x)+xU_m'(x)+\left(\frac{\omega^2\bar{r}^2}{C_L^2}x^2-1-m^2\frac{1-v}{2}\right)U_m(x)$$
$$+\frac{1+v}{2}mxV_m'(x)-\frac{3-v}{2}mV_m(x)=0, \tag{7a}$$

$$x^2V_m''(x)+xV_m'(x)+\left(\frac{\omega^2\bar{r}^2}{C_T^2}x^2-1-m^2\frac{2}{1-v}\right)V_m(x)$$
$$-\frac{1+v}{1-v}mxU_m'(x)-\frac{3-v}{1-v}mU_m(x)=0. \tag{7b}$$

Henceforth, the prime is used to denote differentiation with respect to x.

B. Natural frequencies and mode shapes of the axisymmetric modes ($m=0$)

In the above equations the circumferential wave number m represents the number of nodal diameters in the free vibrational response. The case $m=0$ represents the vibrational modes where u and v are uncoupled. Hence, the uncoupled modes are axisymmetric because there are no nodal diameters. Equations (7) take the following form for the axisymmetric modes ($m=0$):

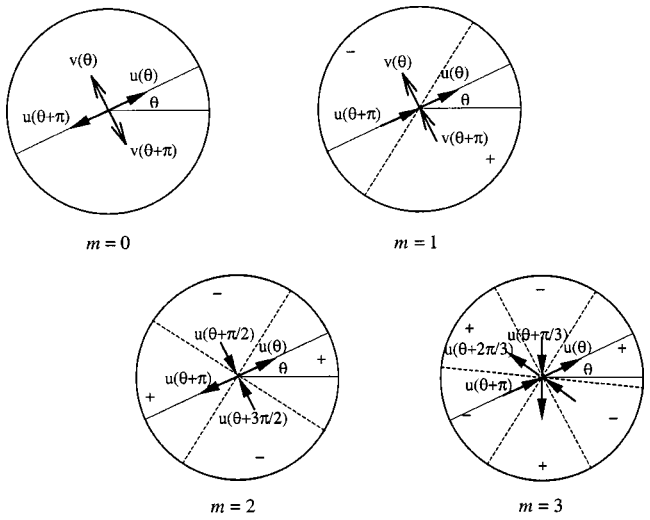

FIG. 2. Free vibration response at the center point of a circular clamped plate for different circumferential wave numbers m (note that for $m=2$ and $m=3$, v is not plotted; it follows the same behavior as u).

$$x^2U_0''(x)+xU_0'(x)+(\lambda_p^2x^2-1)U_0(x)=0, \tag{8a}$$

$$x^2V_0''(x)+xV_0'(x)+(\lambda_q^2x^2-1)V_0(x)=0, \tag{8b}$$

where $\lambda_p^2=\omega^2\overline{r^2}/C_L^2$ and $\lambda_q^2=\omega^2\overline{r^2}/C_T^2$.

Each of Eqs. (8) is a Bessel equation of order unity.[12] Solution of these equations is: $U_{0,p}(x)=J_1(\lambda_p x)$ and $V_{0,q}(x)=J_1(\lambda_q x)$, where $J_1(z)$ is Bessel function of the first kind of order unity. The displacement components must assume zero values at the clamped edge of the plate where $x=1$. Hence, λ_p and λ_q ($=\lambda_p$ in this case) are the roots of the equation: $J_1(z)=0$, excluding the root at the origin. The subscripts p and q stand for the sequential number of the root. Natural frequencies of the radial (extensional) and tangential (torsional) axisymmetric modes are given, respectively, by

$$\omega_{L,p}=\frac{C_L\lambda_p}{\overline{r}} \quad \text{and} \quad \omega_{T,q}=\frac{C_T\lambda_q}{\overline{r}}. \tag{9}$$

Radial distributions of the free vibrational modes take the form of Bessel functions of the first kind of order unity. It has to be stated here that Bessel function of the second kind is also a solution that satisfies Eqs. (8) but it is discarded here because it has a singularity at the origin.[12] In the following analysis, Bessel function of the first kind will be referred to as the Bessel function for brevity.

C. Natural frequencies and mode shapes of the coupled modes ($m>0$)

Although Bessel function of the first order satisfies Eqs. (8) for axisymmetric modes, it does not satisfy Eqs. (7) due to the coupling between the radial, $U(x)$, and tangential, $V(x)$, components of in-plane vibration. However, the radial mode shapes of vibration can be expressed as a series of Bessel functions of any order. The physical in-plane response of the plate at the center $r=0$ has to be examined first to help choosing a function that best represents the behavior at plate center point.

The in-plane response at $r=0$ is examined and presented in Fig. 2, which also depicts the nodal diameters for the first four circumferential wave numbers ($m=0:3$). For $m=0$, if $U(0)$ and $V(0)$ components exist along and normal to any radial direction θ, it will be counteracted by similar response along and normal to the radial direction $\theta+\pi$ due to the axisymmetry. It follows that the axisymmetric mode, $m=0$, must have zero response at the plate center point. This finding agrees with the value of Bessel function of order unity at $x=0$, which is zero.

For $m=1$, it is shown in Fig. 2 that u and v components of the response at $\theta+\pi$ are added to u and v components at θ. This is due to the change of sign of the sine and cosine functions [see Eqs. (3)] when the angle is increased by π. This indicates that the modes $m=1$ have nonzero response at the plate center point.

Figure 2 also presents analysis of the response of the wave numbers $m=2$ and $m=3$ at the center of the plate. Following the same reasoning as before, it is shown that the plate center must have zero response for these two modes. It can also be shown that this always is the case for all the higher order modes ($m\geqslant 4$).

In summary, the modes with circumferential wave number $m=1$ are the only ones that have nonzero response at the center point of the plate.

Radial mode shapes of the modes with circumferential wave numbers $m\geqslant 2$ are assumed as series summations of Bessel functions of integral order $n>0$, which satisfies the condition of zero response at the plate center point

$$U_m(x)=\sum_{p=1}^{\infty}\overline{U}_{m,p}J_n(\lambda_p x), \tag{10a}$$

$$V_m(x)=\sum_{p=1}^{\infty}\overline{V}_{m,p}J_n(\lambda_p x), \tag{10b}$$

where λ_p are nonzero roots of the equation $J_n(z)=0$.

Radial mode shapes of the modes with circumferential wave number $m=1$ are assumed as a series summation of Bessel functions of the order 0.5 divided by $\sqrt{x}$ as follows:

$$U_m(x)=\sum_{p=1}^{\infty}\overline{U}_{m,p}\frac{J_{0.5}(\lambda_p x)}{\sqrt{x}}, \tag{11a}$$

$$V_m(x)=\sum_{p=1}^{\infty}\overline{V}_{m,p}\frac{J_{0.5}(\lambda_p x)}{\sqrt{x}}, \tag{11b}$$

where λ_p are roots of the equation $J_{0.5}(z)=0$.

It can be proved,[12] using expansion of $J_{0.5}(\lambda_p x)$ in terms of x, that $J_{0.5}(\lambda_p x)/\sqrt{x}$ assumes finite value at $x=0$.

Henceforth, $J_{0.5}(\lambda_p x)/\sqrt{x}$ and $J_n(\lambda_p x)$ will be called "elemental mode shapes" for $m=1$ and $m\geqslant 2$, respectively.

1. Natural frequencies and mode shapes of the modes $m\geqslant 2$

Three properties of Bessel functions will be considered in the following analysis:[12]

(a) $U_{m,p}(x)=J_n(\lambda_p x)$ is a solution to the equation

$$x^2U_m''(x)+xU_m'(x)+(\lambda_p^2x^2-n^2)U_m(x)=0. \tag{12}$$

(b) Differentiation of Eq. (10a) is

$$\frac{dU_m}{dx}=\sum_{p=1}^{\infty}\overline{U}_{m,p}\left[\frac{n}{x}J_n(\lambda_p x)-\lambda_p J_{n+1}(\lambda_p x)\right]. \tag{13}$$

(c) The orthogonality of Bessel functions is expressed by the relations

$$\int_{x=0}^{1}xJ_n(\lambda_p x)J_n(\lambda_{p'}x)dx=\begin{cases}0 & p\neq p'\\ \frac{1}{2}[J_{n+1}(\lambda_p)]^2 & p=p'\end{cases}. \tag{14}$$

For brevity and clarity, the subscript m will be removed in the following analysis.

The following equations are obtained after substitution of (10) into (7) and using p' to denote a general elemental mode shape:

$$\sum_{p'=1}^{\infty}a_1J_n(\lambda_{p'}x)\overline{U}_{p'}+\sum_{p'=1}^{\infty}(K_L^2-\lambda_{p'}^2)x^2J_n(\lambda_{p'}x)\overline{U}_{p'}+\sum_{p'=1}^{\infty}a_2J_n(\lambda_{p'}x)\overline{V}_{p'}+\sum_{p'=1}^{\infty}a_3x\lambda_{p'}J_{n+1}(\lambda_{p'}x)\overline{V}_{p'}=0, \tag{15a}$$

$$\sum_{p'=1}^{\infty}b_1J_n(\lambda_{p'}x)\overline{V}_{p'}+\sum_{p'=1}^{\infty}(K_T^2-\lambda_{p'}^2)x^2J_n(\lambda_{p'}x)\overline{V}_{p'}+\sum_{p'=1}^{\infty}b_2J_n(\lambda_{p'}x)\overline{U}_{p'}+\sum_{p'=1}^{\infty}b_3x\lambda_{p'}J_{n+1}(\lambda_{p'}x)\overline{U}_{p'}=0, \tag{15b}$$

where

$$a_1=n^2-1-m^2\frac{1-\nu}{2},\quad b_1=n^2-1-m^2\frac{2}{1-\nu},$$

$$a_2=\frac{1+\nu}{2}mn-\frac{3-\nu}{2}m,\quad b_2=-\frac{1+\nu}{1-\nu}mn-\frac{3-\nu}{1-\nu}m,$$

$$a_3=-\frac{1+\nu}{2}m,\quad b_3=\frac{1+\nu}{1-\nu}m,$$

$$K_L^2=\frac{\omega^2\overline{r^2}}{C_L^2},\quad \text{and}\quad K_T^2=\frac{\omega^2\overline{r^2}}{C_T^2}.$$

Multiplying Eqs. (15) by $[J_n(\lambda_p x)]/x$, integrating with respect to x from $x=0$ to $x=1$, and employing the orthogonality property give rise to the following equations:

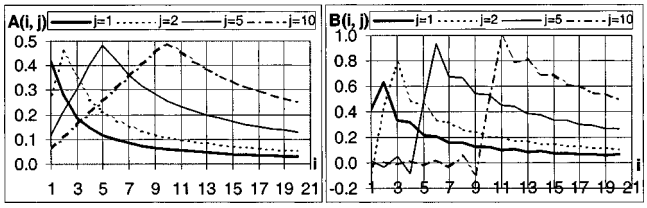

FIG. 3. Modal coupling factors $A_{p',p}$ and $B_{p',p}$ according to Eqs. (17) for $n=1$.

$$a_1\sum_{p'=1}^{\infty}A_{p',p}\overline{U}_{p'}+(K_L^2-\lambda_p^2)C_p\overline{U}_p+a_2\sum_{p'=1}^{\infty}A_{p',p}\overline{V}_{p'}+a_3\sum_{p'=1}^{\infty}B_{p',p}\overline{V}_{p'}=0, \tag{16a}$$

$$b_1\sum_{p'=1}^{\infty}A_{p',p}\overline{V}_{p'}+(K_T^2-\lambda_p^2)C_p\overline{V}_p+b_2\sum_{p'=1}^{\infty}A_{p',p}\overline{U}_{p'}+b_3\sum_{p'=1}^{\infty}B_{p',p}\overline{U}_{p'}=0, \tag{16b}$$

where $C_p=\frac{1}{2}[J_{n+1}(\lambda_p)]^2$,

$$A_{p',p}=\int_{x=0}^{1}\frac{1}{x}J_n(\lambda_{p'}x)J_n(\lambda_p x)dx,$$

$$B_{p',p}=\int_{x=0}^{1}\lambda_{p'}J_{n+1}(\lambda_{p'}x)J_n(\lambda_p x)dx. \tag{17}$$

Equations (16) can be arranged in the form of an eigenvalue problem as follows:

$$K_L^2\overline{U}_p=\left(\lambda_p^2-\frac{a_1}{C_p}A_{p,p}\right)\overline{U}_p-\sum_{\substack{p'=1\\(p'\neq p)}}^{\infty}\frac{a_1}{C_p}A_{p',p}\overline{U}_{p'}-\sum_{p'=1}^{\infty}\frac{a_2A_{p',p}+a_3B_{p',p}}{C_p}\overline{V}_{p'}, \tag{18a}$$

$$K_L^2\overline{V}_p=\left(\lambda_p^2-\frac{b_1A_{p,p}}{C_p}\right)\frac{1-\nu}{2}\overline{V}_p-\sum_{\substack{p'=1\\(p'\neq p)}}^{\infty}\frac{b_1}{C_p}A_{p',p}\frac{1-\nu}{2}\overline{V}_{p'}-\sum_{p'=1}^{\infty}\frac{b_2A_{p',p}+b_3B_{p',p}}{C_p}\frac{1-\nu}{2}\overline{U}_{p'}. \tag{18b}$$

$A_{p',p}$ and $B_{p',p}$ represent the coupling strength between the elemental modes in Eqs. (10). They are plotted in Fig. 3 for different values of p' and p to give a qualitative measure of the expected convergence of the series summation in Eqs. (10). It can be proved that the integrand of $A_{p',p}$ assumes a zero value at $x=0$ for $n>0.5$.

For each circumferential wave number m, Eqs. (18) have to be written for a number, say k, of $U_{m,p}$ and $V_{m,p}$ coupled to $U_{m,p'}$ and $V_{m,p'}$ leading to $2\times k$ equations. The resulting eigenvalue problem can be solved for the eigenvalues (nondimensional frequency parameters K_L) and the eigenvectors

(corresponding mode shapes). The natural frequencies are obtained from the relation $f=(K_L C_L/2\pi\bar{r})$ Hz.

It has to be mentioned here that Chen and Liu,[13] in their solutions for in-plane vibration in plates with free edges, used series summation of Bessel functions of the first kind of order m (m is the circumferential wave number). The mathematical formulation presented in this section uses Bessel functions of integral order $n>0$ (any arbitrary integer). This implies that m may be used as the order of Bessel functions in the series summation in Eqs. (10). However, Bessel functions of order unity were used in the computational examples. It was also confirmed by computational examples (not presented in this paper) that Bessel functions of order m give the same accuracy at the same computational effort [same number of terms in (10) to obtain certain accuracy].

2. Natural frequencies and mode shapes of the modes m=1

The same procedure will be followed in the analysis of this case as for $m\geqslant 2$.

The following properties of Bessel functions are used in the mathematical analysis:[12]

(a) $U_{1,p}(x)=[J_{0.5}(\lambda_p x)/\sqrt{x}]$ is a solution of the equation

$$x^2U_1''(x)+2xU_1'(x)+\lambda_p^2x^2U_1(x)=0. \tag{19}$$

(b) Differentiation of the elemental mode shape in Eqs. (11) is

$$\frac{d}{dx}\left[\frac{J_{0.5}(\lambda_p x)}{x^{0.5}}\right]=-\lambda_p\frac{J_{1.5}(\lambda_p x)}{x^{0.5}}. \tag{20}$$

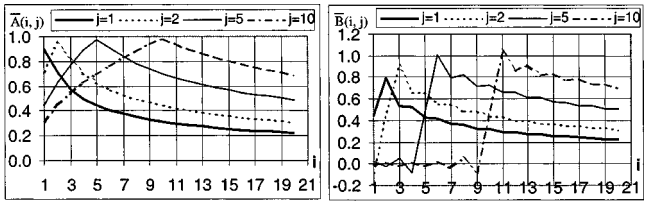

FIG. 4. Modal coupling factors $\bar{A}_{p',p}$ and $\bar{B}_{p',p}$ according to Eqs. (17) for $n=0.5$.

(c) The orthogonality of Bessel functions according to Eqs. (14) is valid for $n=0.5$.

Substitution of the assumed solution from Eqs. (11) into Eqs. (7) gives rise to:

$$\sum_{p'=1}^{\infty}\bar{B}_{p',p}\bar{U}_{p'}+\bar{a}_1\sum_{p'=1}^{\infty}\bar{A}_{p',p}\bar{U}_{p'}+(K_L^2-\lambda_p^2)\bar{C}_p\bar{U}_p+\bar{a}_2\sum_{p'=1}^{\infty}\bar{B}_{p',p}\bar{V}_{p'}+\bar{a}_3\sum_{p'=1}^{\infty}\bar{A}_{p',p}\bar{V}_{p'}=0, \tag{21a}$$

$$\sum_{p'=1}^{\infty}\bar{B}_{p',p}\bar{V}_{p'}+\bar{b}_1\sum_{p'=1}^{\infty}\bar{A}_{p',p}\bar{V}_{p'}+(K_T^2-\lambda_p^2)\bar{C}_p\bar{V}_p+\bar{b}_2\sum_{p'=1}^{\infty}\bar{B}_{p',p}\bar{U}_{p'}+\bar{b}_3\sum_{p'=1}^{\infty}\bar{A}_{p',p}\bar{U}_{p'}=0, \tag{21b}$$

where

TABLE I. Frequency parameters $K_L=\omega\bar{r}/C_L$ (see the list of symbols) for the first eight natural frequencies of the first ten circumferential wave numbers of in-plane vibration in circular clamped plates for two values of poisson's ratio ν=0.28 and ν=0.33.

Wave number	Poisson's ratio	1st mode	2nd mode	3rd mode	4th mode	5th mode	6th mode	7th mode	8th mode
$m=0$, radial	any	3.8317	7.0156	10.1735	13.3237	16.4706	19.6159	22.7601	25.9037
$m=0$, tangential	ν=0.28	2.2990	4.2094	6.1041	7.9942	9.8824	11.7700	13.6560	15.5420
	ν=0.33	2.2178	4.0606	5.8883	7.7116	9.5331	11.3530	13.1730	14.9930
$m=1$	ν=0.28	1.9655	3.2210	5.0696	5.3802	7.0227	8.5254	8.9305	10.8060
	ν=0.33	1.9441	3.1126	4.9104	5.3570	6.7763	8.4938	8.6458	10.4250
$m=2$	ν=0.28	3.0658	4.1344	5.9357	6.7304	7.9147	9.7408	10.0340	11.7070
	ν=0.33	3.0185	4.0127	5.7398	6.7079	7.6442	9.4356	9.9894	11.2970
$m=3$	ν=0.28	3.9956	5.0741	6.7755	7.9853	8.8061	10.6370	11.3680	12.5930
	ν=0.33	3.9116	4.9489	6.5537	7.9342	8.5336	10.2790	11.3380	12.1620
$m=4$	ν=0.28	4.8244	6.0289	7.6072	9.1255	9.7416	11.4966	12.6630	13.4786
	ν=0.33	4.7021	5.8985	7.3648	8.9816	9.5296	11.1087	12.5940	13.0582
$m=5$	ν=0.28	5.5944	6.9753	8.4407	10.1174	10.7708	12.3452	13.8738	14.4020
	ν=0.33	5.4370	6.8306	8.1834	9.8642	10.6324	11.9353	13.6350	14.1196
$m=6$	ν=0.28	6.3301	7.8961	9.2829	11.0012	11.8604	13.1924	14.9187	15.4500
	ν=0.33	6.1410	7.7265	9.0167	10.6837	11.7423	12.7712	14.5015	15.3093
$m=7$	ν=0.28	7.0444	8.7821	10.1376	11.8398	12.9484	14.0485	15.8195	16.6034
	ν=0.33	6.8259	8.5787	9.8666	11.4838	12.8054	13.6373	15.3240	16.4911
$m=8$	ν=0.28	7.7444	9.6309	11.0042	12.6615	13.9993	14.9280	16.6701	17.7658
	ν=0.33	7.4982	9.3887	10.7281	12.2792	13.7879	14.5598	16.1348	17.6027
$m=9$	ν=0.28	8.4340	10.4450	11.8780	13.4780	14.9910	15.8480	17.5050	18.8890
	ν=0.33	8.1612	10.1630	11.5920	13.0770	14.6840	15.5420	16.9450	18.5840
$m=10$	ν=0.28	9.1159	11.2310	12.7500	14.2960	15.9150	16.8120	18.3350	19.9300
	ν=0.33	8.8172	10.9100	12.4470	13.8830	15.5210	16.5510	17.7630	19.4540

$$\bar{a}_1=\bar{a}_3=-\frac{3-\nu}{2},$$

$$\bar{b}_1=\bar{b}_3=-\frac{3-\nu}{1-\nu},$$

$$\bar{a}_2=-\frac{1+\nu}{2},\quad \bar{b}_2=\frac{1+\nu}{1-\nu}.$$

$\bar{C}_p$, $\bar{A}_{p',p}$ and $\bar{B}_{p',p}$ are obtained from relations similar to those of Eqs. (17) with n replaced by 0.5. It can be proved that the integrand of $\bar{A}_{p',p}$ assumes finite value at $x=0$. This is another reason for the choice of the elemental mode shapes in Eqs. (11). Multiplying Eqs. (21) by $J_{0.5}(\lambda_p x)/\sqrt{x}$, integrating with respect to x from $x=0$ to $x=1$, and using the properties of Bessel functions, the following equations are obtained:

TABLE II. Coefficients ($\bar{U}_{m,p}$ and $\bar{V}_{m,p}$) of the elemental modes in $U_{1,p}(\text{or } V_{1,p})=\Sigma_{p=1}^{\infty}\bar{U}_{1,p}(\text{or } \bar{V}_{1,p})[J_{0.5}(\lambda_p x)]/\sqrt{x}$ [Eqs. (11)] and in $U_{m,p}(\text{or } V_{m,p})=\Sigma_{p=1}^{\infty}\bar{U}_{m,p}(\text{or } \bar{V}_{m,p})J_1(\lambda_p x)$ [Eqs. (10), $m\geqslant 2$] for in-plane vibration of circular clamped plate (ν=0.3); the bold numbers highlight the elemental modes with the highest contribution to the radial mode shape.

Circum. wave #	Mode	p 1	2	3	4	5	6	7	8	9	10
$m=1$	#1, $\bar{U}$	**0.7650**	−0.0515	0.0170	−0.0080	0.0046	−0.0028	0.0020	−0.0013	0.0011	−0.0008
	, $\bar{V}$	**−0.6376**	−0.0686	0.0200	−0.0091	0.0051	−0.0031	0.0022	−0.0015	0.0012	−0.0009
	#2, $\bar{U}$	**−0.2197**	−0.1631	0.0257	−0.0107	0.0054	−0.0035	0.0022	−0.0017	0.0011	−0.0010
	, $\bar{V}$	−0.5907	**0.7568**	−0.0473	0.0159	−0.0074	0.0045	−0.0028	0.0020	−0.0014	0.0011
	#3, $\bar{U}$	−0.1133	**0.4293**	0.0940	−0.0153	0.0058	−0.0034	0.0019	−0.0015	0.0009	−0.0009
	, $\bar{V}$	−0.0072	0.4375	**−0.7732**	0.0614	−0.0212	0.0112	−0.0065	0.0045	−0.0031	0.0024
	#4, $\bar{U}$	−0.4573	**0.6097**	−0.1163	0.0243	−0.0113	0.0064	−0.0042	0.0028	−0.0022	0.0015
	, $\bar{V}$	−0.2038	**−0.4850**	0.3566	0.0261	−0.0119	0.0066	−0.0043	0.0028	−0.0022	0.0016
	#5, $\bar{U}$	0.0051	−0.0279	**−0.1971**	−0.0924	0.0165	−0.0077	0.0041	−0.0029	0.0018	−0.0015
	, $\bar{V}$	−0.0252	−0.0643	−0.5233	**0.8186**	−0.0487	0.0170	−0.0081	0.0051	−0.0032	0.0024
$m=2$	#1, $\bar{U}$	**−0.8160**	−0.0176	0.0021	−0.0006	0.0002	−0.0002	0.0000	−0.0001	0.0000	−0.0002
	, $\bar{V}$	**0.5329**	0.2164	−0.0489	0.0212	−0.0117	0.0072	−0.0049	0.0034	−0.0027	0.0019
	#2, $\bar{U}$	0.2670	**0.3034**	−0.0360	0.0146	−0.0078	0.0047	−0.0032	0.0022	−0.0017	0.0012
	, $\bar{V}$	0.5739	**−0.7109**	−0.0180	0.0084	−0.0047	0.0029	−0.0020	0.0014	−0.0012	0.0008
	#3, $\bar{U}$	0.0444	**0.5463**	0.2075	−0.0298	0.0126	−0.0069	0.0044	−0.0030	0.0022	−0.0016
	, $\bar{V}$	−0.0078	0.2578	**−0.7672**	0.0182	−0.0057	0.0027	−0.0016	0.0010	−0.0007	0.0005
	#4, $\bar{U}$	0.3393	**−0.5820**	0.1632	0.0020	0.0007	−0.0004	0.0005	−0.0001	0.0003	0.0001
	, $\bar{V}$	0.3813	**0.5334**	−0.2575	−0.1447	0.0409	−0.0198	0.0119	−0.0077	0.0057	−0.0039
	#5, $\bar{U}$	−0.0033	−0.1766	**−0.3899**	−0.1847	0.0261	−0.0113	0.0064	−0.0040	0.0029	−0.0020
	, $\bar{V}$	−0.0117	−0.0728	−0.3018	**0.8278**	−0.0004	−0.0010	0.0009	−0.0006	0.0006	−0.0004
$m=3$	#1, $\bar{U}$	**−0.8417**	0.2073	0.0753	0.0121	0.0134	0.0032	0.0050	0.0011	0.0022	0.0000
	, $\bar{V}$	**0.4224**	0.1579	−0.1930	0.0228	−0.0337	0.0083	−0.0132	0.0037	−0.0073	0.0013
	#2, $\bar{U}$	−0.2071	**−0.2869**	0.1804	−0.0007	0.0241	−0.0017	0.0088	−0.0011	0.0043	−0.0008
	, $\bar{V}$	**−0.5237**	0.7361	−0.1430	−0.0679	0.0020	−0.0165	0.0022	−0.0073	0.0012	−0.0045
	#3, $\bar{U}$	−0.1359	**−0.5560**	−0.0106	0.1815	0.0096	0.0308	0.0021	0.0118	0.0002	0.0052
	, $\bar{V}$	0.0418	−0.1464	**0.7284**	−0.2858	−0.0419	−0.0255	−0.0107	−0.0092	−0.0058	−0.0059
	#4, $\bar{U}$	−0.2312	**0.4622**	−0.4221	0.0570	0.0384	0.0027	0.0069	0.0003	0.0024	−0.0008
	, $\bar{V}$	−0.4231	−0.3412	**0.4088**	0.2348	−0.1743	0.0265	−0.0303	0.0102	−0.0131	0.0042
	#5, $\bar{U}$	0.0107	0.3265	**0.3505**	0.0053	−0.1776	−0.0175	−0.0323	−0.0051	−0.0126	−0.0010
	, $\bar{V}$	−0.0453	0.0002	0.1537	**−0.7878**	0.2909	0.0730	0.0229	0.0206	0.0093	0.0123
$m=4$	#1, $\bar{U}$	**0.8096**	−0.3702	−0.0668	0.0204	−0.0102	0.0058	−0.0040	0.0028	−0.0020	0.0020
	, $\bar{V}$	**−0.3271**	−0.1188	0.2703	−0.0775	0.0374	−0.0218	0.0144	−0.0096	0.0077	−0.0046
	#2, $\bar{U}$	−0.1635	−0.2873	**0.2925**	−0.0380	0.0172	−0.0099	0.0064	−0.0042	0.0034	−0.0017
	, $\bar{V}$	−0.4647	**0.7186**	−0.2491	−0.0823	0.0370	−0.0210	0.0138	−0.0091	0.0075	−0.0046
	#3, $\bar{U}$	0.1950	**0.4962**	−0.1631	−0.2314	0.0473	−0.0220	0.0131	−0.0083	0.0063	−0.0041
	, $\bar{V}$	−0.0760	0.1053	**−0.6327**	0.4639	−0.0140	0.0025	−0.0005	0.0000	0.0004	−0.0005
	#4, $\bar{U}$	0.1672	−0.1975	**0.5279**	−0.2436	−0.1045	0.0256	−0.0127	0.0074	−0.0051	0.0042
	, $\bar{V}$	0.3667	0.1351	**−0.4147**	−0.2921	0.4077	−0.0721	0.0331	−0.0186	0.0133	−0.0072
	#5, $\bar{U}$	0.0066	**0.4648**	0.1429	−0.1121	−0.2257	0.0359	−0.0169	0.0096	−0.0069	0.0036
	, $\bar{V}$	−0.1635	−0.0490	0.1785	**−0.6596**	0.4463	0.0461	−0.0232	0.0135	−0.0101	0.0059

TABLE II. (*Continued*.)

Circum. wave #	Mode	p 1	2	3	4	5	6	7	8	9	10
$m=5$	#1, $\overline{U}$	**0.7585**	−0.4823	−0.0128	0.0519	−0.0156	0.0116	−0.0068	0.0050	−0.0037	0.0034
	, $\overline{V}$	−0.2621	−0.0821	**0.2984**	−0.1416	0.0506	−0.0318	0.0192	−0.0133	0.0102	−0.0058
	#2, $\overline{U}$	0.1510	0.2845	**−0.3874**	0.1012	−0.0113	0.0123	−0.0054	0.0046	−0.0031	0.0012
	, $\overline{V}$	0.3988	**−0.6788**	0.3167	0.0790	−0.0832	0.0352	−0.0249	0.0151	−0.0129	0.0070
	#3, $\overline{U}$	0.2313	**0.4073**	−0.2783	−0.2132	0.1238	−0.0261	0.0221	−0.0105	0.0096	−0.0050
	, $\overline{V}$	−0.1060	0.1073	−0.5438	**0.5570**	−0.1100	−0.0137	−0.0006	−0.0042	0.0018	−0.0026
	#4, $\overline{U}$	0.1386	0.0266	**0.4357**	−0.4154	−0.0895	0.0950	−0.0193	0.0177	−0.0088	0.0078
	, $\overline{V}$	0.2699	−0.0078	−0.3332	−0.2477	**0.5650**	−0.1845	0.0250	−0.0230	0.0104	−0.0073
	#5, $\overline{U}$	0.0075	**0.5104**	−0.1077	−0.0839	−0.2188	0.1007	−0.0059	0.0132	−0.0044	0.0028
	, $\overline{V}$	−0.2789	−0.0155	0.2504	**−0.5582**	0.4490	0.0176	−0.0832	0.0280	−0.0261	0.0105
$m=6$	#1, $\overline{U}$	**−0.7048**	0.5568	−0.0609	−0.0657	0.0291	−0.0162	0.0110	−0.0071	0.0059	−0.0048
	, $\overline{V}$	0.2181	0.0484	**−0.2954**	0.1954	−0.0754	0.0408	−0.0255	0.0168	−0.0131	0.0067
	#2, $\overline{U}$	0.1594	0.2677	**−0.4645**	0.1798	−0.0148	0.0076	−0.0042	0.0030	−0.0021	−0.0002
	, $\overline{V}$	0.3328	**−0.6238**	0.3563	0.0675	−0.1307	0.0615	−0.0365	0.0235	−0.0185	0.0099
	#3, $\overline{U}$	−0.2507	−0.3128	**0.3341**	0.1679	−0.1900	0.0511	−0.0264	0.0158	−0.0116	0.0064
	, $\overline{V}$	0.1296	−0.1311	0.4805	**−0.5940**	0.2041	0.0111	−0.0109	0.0078	−0.0069	0.0043
	#4, $\overline{U}$	−0.1318	−0.1279	−0.2973	**0.5067**	−0.0027	−0.1493	0.0453	−0.0228	0.0157	−0.0097
	, $\overline{V}$	−0.2125	0.0858	0.2568	0.1485	**−0.5953**	0.3138	−0.0457	0.0191	−0.0109	0.0042
	#5, $\overline{U}$	−0.0257	**−0.4727**	0.2438	0.0082	0.2333	−0.1591	0.0061	−0.0041	0.0021	0.0016
	, $\overline{V}$	0.3222	−0.0647	−0.2411	**0.5080**	−0.4291	−0.0188	0.1481	−0.0635	0.0401	−0.0190
$m=7$	#1, $\overline{U}$	**−0.6541**	0.6044	−0.1386	−0.0599	0.0441	−0.0224	0.0154	−0.0097	0.0084	−0.0064
	, $\overline{V}$	0.1869	0.0197	**−0.2754**	0.2329	−0.1063	0.0521	−0.0322	0.0210	−0.0160	0.0077
	#2, $\overline{U}$	0.1771	0.2356	**−0.5183**	0.2645	−0.0318	−0.0013	−0.0006	0.0004	0.0002	−0.0022
	, $\overline{V}$	0.2714	**−0.5598**	0.3748	0.0500	−0.1721	0.0973	−0.0510	0.0328	−0.0246	0.0124
	#3, $\overline{U}$	−0.2580	−0.2258	**0.3449**	0.1231	−0.2397	0.0907	−0.0325	0.0204	−0.0138	0.0070
	, $\overline{V}$	0.1447	−0.1599	0.4410	**−0.6008**	0.2787	−0.0043	−0.0280	0.0160	−0.0140	0.0076
	#4, $\overline{U}$	−0.1312	−0.1681	−0.1716	**0.5349**	−0.1177	−0.1665	0.0862	−0.0307	0.0225	−0.0121
	, $\overline{V}$	−0.1822	0.1348	0.1869	0.0627	**−0.5584**	0.4200	−0.0976	0.0164	−0.0101	0.0019
	#5, $\overline{U}$	0.0526	**0.4144**	−0.2830	0.0369	−0.2747	0.2310	−0.0138	−0.0152	0.0058	−0.0079
	, $\overline{V}$	−0.3147	0.1366	0.1657	**−0.4616**	0.4284	0.0347	−0.2310	0.1203	−0.0571	0.0259
$m=8$	#1, $\overline{U}$	−0.6078	**0.6327**	−0.2122	−0.0384	0.0554	−0.0305	0.0201	−0.0128	0.0112	−0.0081
	, $\overline{V}$	0.1636	−0.0035	−0.2474	**0.2548**	−0.1376	0.0668	−0.0394	0.0258	−0.0190	0.0086
	#2, $\overline{U}$	−0.1959	−0.1919	**0.5457**	−0.3464	0.0635	0.0093	−0.0063	0.0032	−0.0038	0.0046
	, $\overline{V}$	−0.2182	**0.4939**	−0.3789	−0.0264	0.2012	−0.1371	0.0696	−0.0425	0.0308	−0.0145
	#3, $\overline{U}$	0.2572	0.1536	**−0.3297**	−0.0904	0.2773	−0.1377	0.0434	−0.0235	0.0155	−0.0067
	, $\overline{V}$	−0.1501	0.1818	−0.4155	**0.5933**	−0.3319	0.0240	0.0471	−0.0305	0.0235	−0.0121
	#4, $\overline{U}$	0.1310	0.1812	0.0662	**−0.5191**	0.2240	0.1494	−0.1295	0.0472	−0.0291	0.0152
	, $\overline{V}$	0.1646	−0.1692	−0.1192	−0.0076	**0.4945**	−0.4909	0.1660	−0.0225	0.0061	−0.0001
	#5, $\overline{U}$	0.0819	**0.3527**	−0.2641	0.0293	−0.3111	0.3205	−0.0340	−0.0453	0.0242	−0.0159
	, $\overline{V}$	−0.2731	0.1775	0.0588	−0.3823	**0.4260**	0.0490	−0.3280	0.2013	−0.0792	0.0288

$$K_L^2\overline{U}_p=\left(\lambda_p^2-\frac{\overline{B}_{p,p}+\overline{a}_1\overline{A}_{p,p}}{C_p}\right)\overline{U}_p-\sum_{\substack{p'=1\\(p'\neq p)}}^{\infty}\frac{\overline{B}_{p',p}+\overline{a}_1\overline{A}_{p',p}}{C_p}\overline{U}_{p'}-\sum_{p'=1}^{\infty}\frac{\overline{a}_2\overline{B}_{p',p}+\overline{a}_3\overline{A}_{p',p}}{C_p}\overline{V}_{p'},\tag{22a}$$

$$K_L^2\overline{V}_p=\left(\frac{\lambda_p^2}{\frac{2}{1-\nu}}-\frac{\overline{B}_{p,p}+\overline{b}_1\overline{A}_{p,p}}{\overline{C}_p\frac{2}{1-\nu}}\right)\overline{V}_p-\sum_{\substack{p'=1\\(p'\neq p)}}^{\infty}\frac{\overline{B}_{p',p}+\overline{b}_1\overline{A}_{p',p}}{\overline{C}_p\frac{2}{1-\nu}}\overline{V}_{p'}-\sum_{p'=1}^{\infty}\frac{\overline{b}_2\overline{B}_{p',p}+\overline{b}_3\overline{A}_{p',p}}{\overline{C}_p\frac{2}{1-\nu}}\overline{U}_{p'}.\tag{22b}$$

TABLE III. Comparisons of natural frequency predictions by the present method and by Finite Element Analysis for the plate described in Sec. III ("p" is number of terms in the series summation; "e" is total number of finite elements). (a) Axisymmetric modes, circumferential wave number $m=0$. (b) Circumferential wave number, $m=1$. (c) Circumferential wave numbers, $m=2$ and $m=3$. (d) Circumferential wave numbers, $m=7$ and $m=8$.

(a)	$m=0$, tangential modes					$m=0$, radial modes			
Mode number	Eqs. (8)		Finite element		Mode number	Eqs. (8)		Finite element	
	Hz	p	Hz	e		Hz	p	Hz	e
1	3 860	1	3 868	1 200	1	6 434	1	6 439	1 200
			3 863	3 000				6 437	3 000
2	7 068	1	7 101	1 200	2	11 780	1	11 822	1 200
			7 084	3 000				11 807	3 000
3	10 249	1	10 347	1 200	3	17 082	1	17 229	1 200
			10 304	3 000				17 175	3 000
4	13 423	1	13 644	1 200					
			13 553	3 000					
5	16 593	1	17 014	1 200					
			16 849	3 000					

(b)	Eqs. (23)		Finite element			Eqs. (22)		Finite element	
Mode number	Hz	p	Hz	e	Mode number	Hz	p	Hz	e
1	3 301	5	3 303	1 200	6	14 321	5	14 398	1 200
	3 300	10	3 301	3 000		14 314	10	14 365	3 000
	3 300	20				14 315	20		
2	5 420	5	5 425	1 200	7	14 908	5	15 292	1 200
	5 406	10	5 416	3 000		15 001	10	15 176	3 000
	5 408	20				14 995	20		
3	8 484	5	8 558	1 200	8		5	18 691	1 200
	8 517	10	8 538	3 000		18 137	10	18 485	3 000
	8 512	20				18 144	20		
4	9 036	5	9 063	1 200	9	19 653	5		
	9 034	10	9 047	3 000		19 658	10	19 793	3 000
	9 034	20				19 657	20		
5	11 831	5	11 939	1 200					
	11 787	10	11 879	3 000					
	11 792	20							

(c)	$m=2$				$m=3$			
Mode number	Eqs. (18)		Finite element		Eqs. (18)		Finite element	
	Hz	p	Hz	e	Hz	p	Hz	e
1	5 149	5	5 155	1 200	6 710	10	6 729	1 200
	5 148	10	5 151	3 000	6 709	20	6 716	3 000
	5 148	20			6 709	30		
2	6 943	5	6 976	1 200	8 520	10	8 583	1 200
	6 942	10	6 956	3 000	8 520	20	8 542	3 000
	6 942	20			8 520	30		
3	9 969	5	10 048	1 200	11 378	10	11 489	1 200
	9 967	10	10 013	3 000	11 377	20	11 435	3 000
	9 967	20			11 376	30		
4	11 304	5	11 351	1 200	13 409	10	13 504	1 200
	11 301	10	11 323	3 000	13 408	20	13 450	3 000
	11 301	20			13 408	30		
5	13 295	5	13 486	1 200	14 790	10	15 015	1 200
	13 290	10	13 410	3 000	14 786	20	14 922	3 000
	13 289	20			14 786	30		
6	16 368	5	16 648	1 200	17 868	10	18 306	1 200
	16 356	10	16 544	3 000	17 861	20	18 139	3 000
	16 356	20			17 861	30		
7	16 862	5	17 060	1 200				
	16 849	10	16 970	3 000				
	16 848	20						

$\overline{A}_{p',p}$ and $\overline{B}_{p',p}$ represent the coupling strength between the elemental modes in Eqs. (11). They are plotted in Fig. 4 for different values of p' and p to give a qualitative measure of the expected convergence of the series summation in Eqs. (11). $\overline{C}_p$ is the same as in Eq. (17) with $n=0.5$.

Solution of the eigenvalue problem of Eqs. (22) will produce the frequency parameters K_L and the mode shapes.

Table I is a tabulation of the frequency parameters for

TABLE III. (*Continued*.)

(d) Mode number	$m=7$				$m=8$			
	Eqs. (18)		Finite element		Eqs. (18)		Finite element	
	Hz	p	Hz	e	Hz	p	Hz	e
1	11 832	10	12 090	1 200	13 009	10	13 367	1 200
	11 828	20	11 891	3 000	13 003	20	13 094	3 000
2	14 751	10	15 152	1 200	16 179	10	16 718	1 200
	14 746	20	14 857	3 000	16 171	20	16 323	3 000
3	17 028	10	17 484	1 200	18 486	10	19 077	1 200
	17 022	20	17 172	3 000	18 477	20	18 668	3 000
4	19 889	10						
	19 880	20	20 158	3 000				

the first eight modes of circumferential wave numbers $m=0$ to $m=10$. The frequency parameters are calculated for two values of Poisson's ratio $\nu=0.28$ and $\nu=0.33$ representing typical values for steel and aluminum, respectively. Coefficients of the elemental modes in Eqs. (11) and (10), are listed in Table II (calculated for $\nu=0.3$). Mode shapes are depicted in Table V as part of the computational example.

III. COMPUTATIONAL RESULTS AND COMPARISONS

In this section: (i) The natural frequencies and mode shapes are computed using the procedures of Sec. II. (ii) The results are compared with finite-element analysis predictions and with previously published data to assess the accuracy of the new method. (iii) Effect of the number of terms in the series summation of Eqs. (10) and (11) on the accuracy of the results is investigated. (iv) The effect of Poisson's ratio on the natural frequencies is examined computationally. (v) The effect of plate thickness is discussed. The procedures presented in Sec. II are used to compute the natural frequencies and mode shapes of for a 1-m-diameter circular thin plate clamped at the outer edge. MATLAB programming and eigenvalue solutions were used. The plate is made of steel of Young's modulus $E=200\times10^9$ N/m^2, density $\rho=7800$ kg/m^3, and Poisson's ratio $\nu=0.28$. Finite-element analysis (FEA) was also used to compute the natural frequencies and mode shapes for comparison and assessment of the accuracy of the new method. Membrane shell elements were used in the finite-element analysis and two axisymmetric mesh models were built: (1) 1200-element mesh, 20 elements along the radius and 60 elements along the circumference; (2) 3000-element model, 25 elements along the radius and 120 element along the circumference.

Tables III(a)–(d) summarize the results of the numerical computations of the in-plane natural frequencies of the plate in the frequency range up to 20 kHz.

It is expected that the accuracy of the predictions of the present method will depend upon the number of terms used in the series summation of Eqs. (10) and (11). The predictions listed in Tables III(a)–(d) indicate that ten terms in the series summation are sufficient for accuracy to three significant figures.

The accuracy of FE predictions decreases as the frequency increases (for the same number of elements). In particular, FE predictions are less accurate for the modes with large number of nodal diameters (i.e., large circumferential wave number m). It is clear from Tables III(a)–(d) that FE accuracy increased when the number of elements along the circumference was increased from 60 in the first mesh model to 120 in the second mesh model. It is also evident that FE predictions are always higher than the predictions of the present method. At low frequencies, i.e., lower circumferential wave numbers and lower-order modes, predictions of the present method and of FE are nearly identical. Consequently, the deviations at higher frequencies and for higher-order modes are judged to be due to insufficient number of elements in the FE mesh model.

It can be noted from Table I that the frequency parameters for the radial axisymmetric modes ($m=0$) are independent of Poisson's ratio because the radial and tangential components of in-plane response are uncoupled as explained in Sec. II B. On the contrary, the natural frequency of any asymmetric mode ($m>0$) decreases as Poisson's ratio increases. Similar behavior is reported in Ref. 8 for free disks. Calculations of frequency parameters in Table I are based on 20 terms in the series summation of Eqs. (10) and (11), which ensures accuracy to four significant figures. Comparisons with the results of Ref. 10 are presented in Table IV. It can be seen that the agreement is at least to three significant figures. The difference in the second line, between 7.013 and 7.0156, is worth comment. The present solution, for this case, is exact as indicated in Sec. II B and the frequency

TABLE IV. Comparisons of frequency parameters with the results of Ref. 10 ($\nu=0.3$ was used to calculate frequency parameters for $m>0$ (radial)).

Circumferential wave number	Irie *et al.*, Ref. 10	Present work
$m=0$	3.831	3.8317
(radial)	7.013	7.0156
$m=0$	2.267	2.2669
(tangential)	4.151	4.1505
$m=1$	1.958	1.9571
	3.180	3.1781
$m=2$	3.046	3.0474
	4.085	4.0859
$m=3$	3.964	3.9631
	5.024	5.0239
$m=4$	4.777	4.7768
	5.977	5.9767

TABLE V. Tabulation of the mode shapes, solid lines $U_{m,p}$, dashed lines $V_{m,p}$.

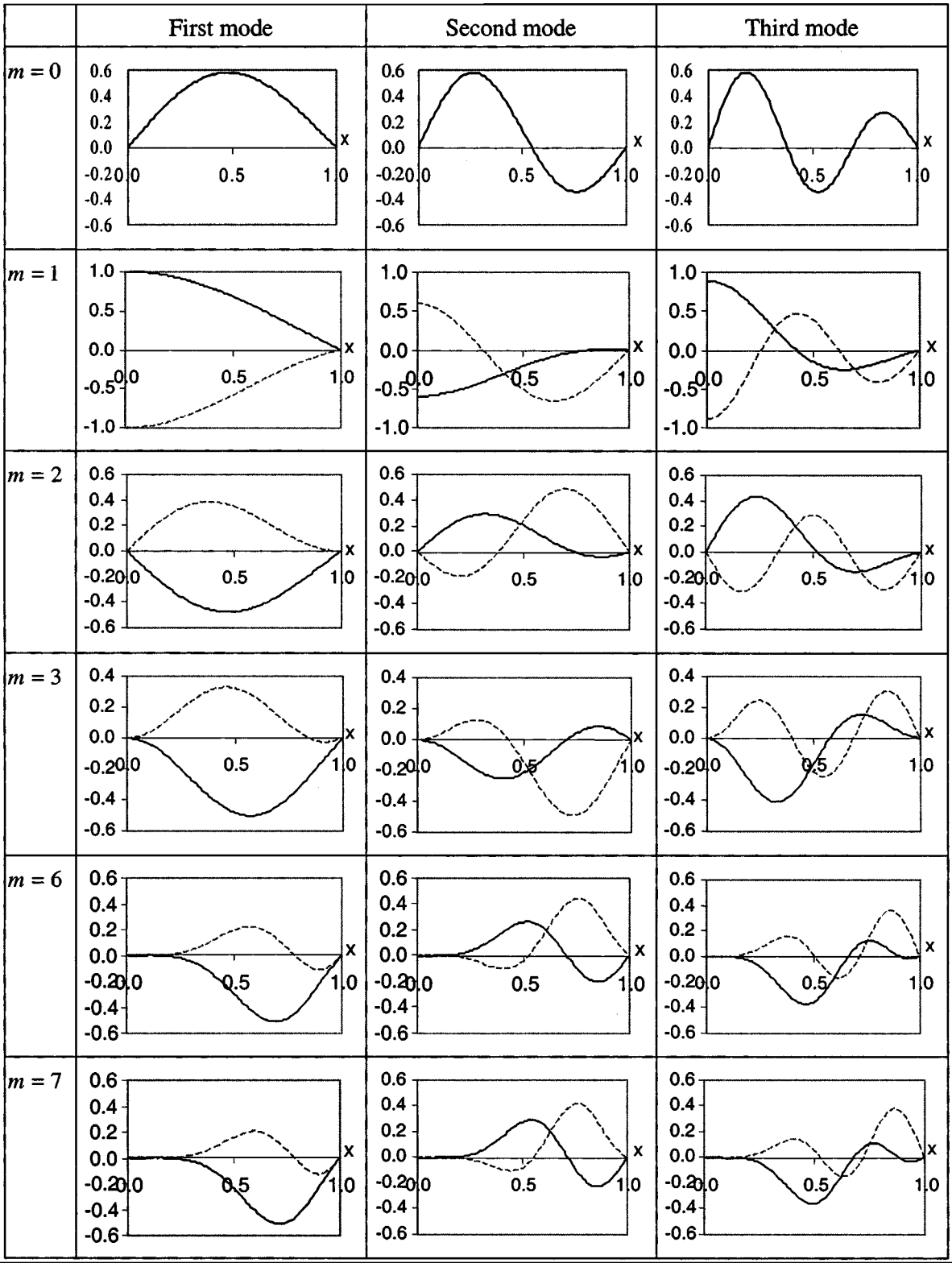

parameter computed by the present method is the second nonzero root of the equation $J_1(z)=0$.

The thickness of the plate is not appearing in the frequency equations [see Eqs. (8), (18) and (22)], implying that it has no effect on the free in-plane vibrational response of the plate. This is only true in the range of validity of Eqs. (1). This issue has been investigated and discussed in detail in Ref. 14. It is shown, in Ref. 14, that the results of the two-dimensional plane stress equations [Eqs. (1)] are accurate in the frequency range where the frequency of the first thickness mode is much higher than the highest in-plane natural frequency in the range. The first thickness mode occurs when the plate thickness equals a half wavelength [see Eq. (29) in Ref. 14]. The coupling between the thickness modes and

in-plane modes increases as the two approach each other. Numerical and experimental results reported in Ref. 14 show that the effect of coupling between the fundamental thickness mode and the in-plane modes starts to diminish rapidly as the thickness to diameter ratio decreases to less than 0.2. In the transportation structures, of interest in this study, this ratio is usually far less than 0.2, indicating that the results of the present analysis are expected to be accurate through the frequency range of interest which is probably up to 20 kHz.

Radial distribution of the mode shapes are depicted in Table V for the first three modes of circumferential wave numbers $m=0$, 1, 2, 3, 6, and 7. It can be seen that the number of nodal circles is not always the same for the radial and tangential components of in-plane vibration of a mode. Also, a node of one component at a certain point is not necessarily associated with an antinode for the orthogonal component. In general, lower-order modes have more movement near the plate center, while higher-order modes have more movement near the clamped edge.

IV. CONCLUSIONS

The modal characteristics of in-plane vibration in circular thin flat plates with clamped edge are investigated in this work. The equations of in-plane vibration are solved for the natural frequencies and mode shapes. Assumed mode shapes are expressed in terms of trigonometric functions in the circumferential direction. It is proved that the circumferential modes are completely uncoupled. This means that the displacement components in the tangential and in the radial directions always have the same mode shape in the circumferential direction, though shifted by $\pi/2m$ where m is the circumferential wave number representing the number of nodal diameters [see Eqs. (3)].

It is shown that the modes with circumferential wave number equal to unity $(m=1)$ are the only modes with displacement at the plate center point. All other modes have zero motion at the plate center point. As a consequence, only a combination of modes with $m=1$ is expected to constitute the response of the plate to in-plane excitation at the center point of the circular clamped plate.

It is proved that the mode shapes, in the radial direction, for the axisymmetric modes $(m=0)$, are Bessel functions of the first type of order unity. Mode shapes in the radial direction for $m=1$ are assumed as series summation of elemental mode shapes of the form $J_{0.5}(\lambda_p x)/\sqrt{x}$ to suit the finite response at the plate center point. Mode shapes in the radial direction for $m \geqslant 2$ are assumed as series summation of elemental mode shapes of the form $J_n(\lambda_p x)$ that represent the physical behavior of zero response at the plate center point.

The mathematical solution for free vibration is written in the form of an eigenvalue problem so that natural frequencies and modes shapes can be obtained by solving for the eigenvalues and the eigenvectors employing any suitable mathematical software. The frequency parameters (nondimensional natural frequencies) obtained by the present method are tabulated and the mode shapes are depicted to illustrate the free-vibration behavior in the frequency range of practical interest. Accuracy of the predictions of natural frequencies and mode shapes is assessed by comparisons with finite-element predictions and with previously reported results. The present method gives very accurate predictions. Effect of Poisson's ratio on the natural frequencies has also been examined. Natural frequency of the radial axisymmetric modes $(m=0)$ is independent of Poisson's ratio, while the natural frequency of any other mode decreases as Poisson's ratio increases. Extension of the present solution to the case of elastically restrained edges, which practically is more realistic, is a possibility for future work.

[1] A. Leissa, *Vibration of Plates* (Acoustical Society of America, Woodbury, NY, 1993).
[2] R. D. Blevins, *Formulas for Natural Frequency and Mode Shape* (Krieger, Malabar, FL, 1995).
[3] N. H. Farag and J. Pan, "Modal characteristics of in-plane vibration of rectangular plates," J. Acoust. Soc. Am. **105**, 3295–3310 (1999).
[4] N. H. Farag and J. Pan, "Free and forced in-plane vibration of rectangular plates," J. Acoust. Soc. Am. **103**, 408–413 (1998).
[5] J. So and A. W. Leissa, "Three-dimensional vibrations of thick circular and annular plates," J. Sound Vib. **209**(1), 15–41 (1998).
[6] R. M. Grice and R. J. Pinnington, "Vibration analysis of a thin-plate box using a finite element model which accommodates only in-plane motion," J. Sound Vib. **232**(2), 449–471 (2000).
[7] C. F. Liu and Y. T. Lee, "Finite element analysis of three-dimensional vibrations of thick circular and annular plates," J. Sound Vib. **233**(1), 63–80 (2000).
[8] R. Holland, "Numerical studies of elastic-disk contour modes lacking axial symmetry," J. Acoust. Soc. Am. **40**, 1051–1057 (1966).
[9] G. Ambati, J. F. W. Bell, and J. C. K. Sharp, "In-plane vibrations of annular rings," J. Sound Vib. **47**(3), 415–432 (1976).
[10] T. G. Irie, Yamada, and Y. Muramoto, "Natural frequencies of in-plane vibration of annular plates," J. Sound Vib. **97**(1), 171–175 (1984).
[11] J. S. Chen and J. L. Jhu, "On the in-plane vibration and stability of a spinning annular disk," J. Sound Vib. **195**(4), 585–593 (1996).
[12] O. J. Farrell and B. Ross, *Solved Problems: Gamma and Beta Functions, Legendre Polynomials, Bessel Functions* (Macmillan, New York, 1963).
[13] S. S. H. Chen and T. M. Liu, "Extensional vibration of thin plates of various shapes," J. Acoust. Soc. Am. **58**, 828–831 (1975).
[14] T. R. Kane and R. D. Mindlin, "High-frequency extensional vibrations of plates," J. Appl. Mech. **23**, 277–283 (1956).